Catastrophe Risk Management Incorporating Natural Climate Cycles and Global Warming

Chia-Chien Chang

Associate Professor, Department of Finance,
National Kaohsiung University of Applied Science, Taiwan

Jen-Wei Yang

Doctoral Candidate, Department of Finance,
National Taiwan University, Taiwan

Min-Teh Yu*

Professor, Institute of Finance,
National Chiao Tung University, Taiwan

June. 12th, 2014

* Chang: Tel.: 886-7-3814526, Fax: 886-7-3831544, Email: cchiac@kuas.edu.tw; Yang: Tel.: 886-7-3814526, Fax: 886-7-3831544, E-mail: dor1214@hotmail.com; Chuang: Email: hlchuang@mx.nthu.edu.tw; and Yu: Tel.: 886-2-33661096, Fax: 886-2-23660764, Email: mtyu@nctu.edu.tw. Corresponding author: Yu. The authors thank the helpful comments from Edward M. H. Lin and Yu-Ren Wang.

Catastrophe Risk Management Incorporating Natural Climate Cycles and Global Warming

Abstract

This paper develops a regime-switching compound Poisson process in which the state of hurricane intensity is a function of the forecast values of the Atlantic Multidecadal Oscillation (AMO) and carbon dioxide (CO_2) indices. Our empirical results demonstrate the asymmetric effect of the AMO index and the CO_2 index on U.S. hurricane intensity. The resulting regime-switching model incorporating the AMO and CO_2 (RACM) provides an excellent projection of the annual U.S. hurricane frequency with a forecasting error of about one. We also examine the influence of the regime-switching effect, the AMO effect and the CO_2 effect on the tail value at risk (TailVaR) of hurricane risk and reinsurance premiums, and find that the RACM model can effectively manage the hurricane risk by setting appropriate reserves. Pricing errors resulting from utilizing the RACM for stop-loss reinsurance premiums are 55 to 70 percent smaller than those from the linear constant model. Furthermore, the regime-switching effect and the AMO effect dominate the CO_2 effect in reducing pricing errors and producing more effective TailVaR, and the CO_2 has its largest effect in 2008—the year of Hurricane Ike.

Keywords: Regime-switching compound Poisson process, Hurricane intensity, AMO index, CO_2 index; Reinsurance premium.

Catastrophe Risk Managements Incorporating Natural Climate Cycle and Global Warming

1. Introduction

Catastrophes (CAT) occur infrequently but often lead to severe losses. A report from the Insurance Information Institute indicates that U.S. hurricanes and tropical storms were responsible for 44% of the total losses associated with CAT events from 1991 to 2010. The most costly insured CAT losses in the U.S. are resulted from weather-related CAT, in particular, hurricanes. (See Table 1). For better risk management of hurricane events and more accurate valuation of CAT insurance products, it is thus important to have reliable forecasts generated from hurricane intensity models.

[Table 1 is here]

Questions remain about the factors that cause increased hurricane activities. Recent meteorological studies (e.g., Lehmiller et al., 1997; Bove et al., 1998; Maloney and Hartmann, 2000; Elsner et al., 2000; Goldenberg et al., 2001; Landsea, 2005; Sutton and Hodson 2005) attribute increases in Atlantic hurricane activity to natural climate cycles, including the Atlantic Multidecadal Oscillation (AMO), the El Nino-Southern Oscillation (ENSO) and the North Atlantic Oscillation (NAO)[1]. Geo Risks Research at Munich Reinsurance has performed hurricane frequency analyses that account for the AMO in recent decades. The AMO index—which measures sea surface temperature (SST) anomalies of the North Atlantic that are correlated with hurricane activity—has been used to predict near-term hurricane activity. Warm phases in the AMO (i.e., a positive AMO index) may lead to higher SSTs and above-average hurricane activity over the long term in the Atlantic. Cool phases in the AMO (negative AMO index) may lead to lower SSTs and below-average hurricane activity over the

[1] The ENSO measures temperature anomalies in the Pacific Ocean off the coast of Peru; and the NAO is a north-south shift (or vice versa) in the track of storms and depressions across the North Atlantic Ocean and into Europe.

long term.

However, other studies (Knutson and Tuleya 2004; Barnett et al. 2005; Emanuel, 2005; Webster et al., 2005; Webster et al. 2006) suggest that global climate change—rather than natural climate cycles—is playing the dominant role in generating higher levels of hurricane activity. The fourth status report of the Intergovernmental Panel on Climate Change (IPCC 2007) indicates that there may be a significant link between human-induced global warming and the greater frequency and intensity of unanticipated tropical cyclone events. Storm frequencies during the current warm phase (since 1995) have been much higher than during the previous warm phases that occurred during the middle of the last century. These frequency differences cannot easily be explained by natural fluctuations. Instead, this difference can be attributed to human-induced global warming; thus, the AMO index and human-induced global warming may have an asymmetric effect on hurricane intensity. Human-induced global warming is caused by an increase in the atmospheric levels of greenhouse gases and aerosols, in solar radiation and in land surface properties. Carbon dioxide (CO_2) is the most important anthropogenic greenhouse gas, and increased CO_2 levels are primarily the result of fossil fuel use and changes in land use. Certain empirical studies (e.g., Henderson-Sellers et al. 1998, Knutson and Tuleya 2004) suggest that doubling CO_2 production increases the frequency of the most intense hurricane events.

Meteorologists such as Elsner et al. (1993, 2000, 2001, 2003, 2006) among others (Solow and Moore 2000; Jagger et al. 2002; and McDonnell and Holbrook 2004) have used the Poisson regression model to forecast hurricane intensity. The Poisson regression, which is a linear regression variant, is appropriate for modeling the influence of a set of independent natural climate cycle variables on the expected rate of a Poisson distributed random process, and it is used to characterize North Atlantic hurricane activity[2]. Elsner et al. (2008) utilize a

[2] See Elsner and Schmertmann 1993; Elsner et al. 2001; Elsner and Bossak 2004; Briggs 2008; Elsner et al. 2008

linear Poisson regression model to forecast North Atlantic hurricane intensity based on the predicted coefficients of the Atlantic SST model. However, the research of Elsner et al. (2008) has its limitations because it uses one-state hurricane intensity and does not respond to global warming information.

Insurance economists however, based on data of CAT losses, employ a compound Poisson process to describe CAT intensity to price insurance products (e.g., Cummins and Geman, 1995; Louberge et al., 1999; Lee and Yu, 2002; Cox et al., 2004; Jaimungal and Wang, 2006). Lin, Chang, and Powers (2009) point out the deterministic intensity of the compound Poisson process is inadequate for natural CAT events and propose a doubly stochastic Poisson process to model the intensity process. Wu and Chung (2010) reinvestigate the intensity process of CAT occurrence and adopt a mean-reverting process for the CAT intensity. Chang, Lin, and Yu (2011) derive a pricing formula for CAT equity put options by assuming that hurricane events follow a continuous-time Markov-modulated Poisson process. Models of economists build upon loss data and fail to evaluate or incorporate important climate variables, such as AMO and CO_2 indices. These models are also generally incapable of forecasting future weather-related CAT intensity.

This paper connects the meteorology and the insurance economics literatures and makes the following contributions. First, we provide a general regime-switching compound Poisson (RSCP) process to capture the characteristics of two-state hurricane intensity. This process also allows greater flexibility and predictive power regarding hurricane intensity by incorporating both natural climate and global warming variables. Second, we utilize data for AMO and CO_2 that are available from the National Oceanic and Atmospheric Administration and data for hurricane frequency and losses that are available from the U.S. database on spatial hazard events and losses. Employing these data, we obtain the predicted values for the AMO and CO_2 indices using the ARMA model and combine with the RSCP model to forecast U.S. hurricane intensity. Our empirical results show that the regime-switching model

that incorporates the AMO and CO_2 effects (RACM) improve it projection of the average annual U.S. hurricane frequency substantially, with a forecasting error of about one.

For the management of hurricane risk, we further examine the influence of the regime-switching effect, the AMO effect and the CO_2 effect on the tail value at risk (TailVaR) and stop-loss reinsurance premiums. Finally, we offer a measure that is equivalent to the physical measure in the RSCP model by employing the discrete-time Esscher transform method to provide a closed-form solution for weather-induced CAT reinsurance premiums for insurance practitioners and compare pricing errors with previous pricing models. Our results provide insurers the appropriate reserves to manage hurricane risk based on the RACM developed in this study. The pricing errors of reinsurance premium using the RACM are 55 to 70 percent smaller than those found using the linear constant model (LM). Furthermore, the regime-switching effect and the AMO effect dominate the CO_2 effect. However, the CO_2 effect is still effective in reducing pricing error and estimating TailVaR, especially in the year of Hurricane Ike, 2008. Our empirical and analytic results support our inclusion of regime-switching effect, the CO_2 effect, and the AMO effect in forecasting hurricane activity and pricing weather-induced CAT products.

The remainder of the paper is organized in the following manner. Section 2 presents the RSCP model and the time series model of the AMO and CO_2 indices. Section 3 provides the empirical analysis for the AMO and CO_2 indices and the goodness of fit of hurricane intensity for the different models. Section 4 introduces TailVaR and the pricing of weather-induced CAT stop-loss reinsurance, and investigates the impact of the regime-switching effect, the AMO effect and the CO_2 effect on them. Section 5 provides conclusions.

2. Modeling: Regime-switching compound Poisson process

This section extends the compound Poisson process to a regime-switching compound

Poisson (RSCP) process to model total CAT losses. Let Y_t be the aggregate losses from CAT events from time $t-1$ to t,

$$Y_t = \sum_{n=N_{t-1}}^{N_t} y_n \tag{1}$$

where y_n describes the inflation-adjusted loss from a weather-induced CAT at time n, which is a sequence of independent and identically distributed positive random variables. The popular distribution of y_n includes exponential distribution, gamma distribution, Weibull distribution and lognormal distribution. N_t denotes the counts of weather-induced CAT events at time t, which represents a Poisson process with the intensity parameter λt that is independent of all other random variables.

In order to include the influence of natural climate cycles and global warming on weather-induced CAT intensity, we propose a RSCP model to capture the aggregate losses from CAT events from time $t-1$ to t, as follows:

$$Y_t = \begin{cases} \sum_{n=N_{t-1,1}}^{N_{t,1}} y_n = Y_{t,1} & if \quad S_t = 1, \\ \sum_{n=N_{t-1,2}}^{N_{t,2}} y_n = Y_{t,2} & if \quad S_t = 2, \end{cases} \tag{2}$$

where $S_t = 1$ is the high CAT event state and $S_t = 2$ is the low CAT event state. The state variable $S_t = \{1, 2\}$ is assumed to follow a first-order Markov process and state transition probabilities given the $t-1$ information F_{t-1} are as follows:

$$p(S_t = 1 | S_{t-1} = 1,\ F_{t-1}) = p_{11}, \tag{3}$$

$$p(S_t = 2 | S_{t-1} = 2,\ F_{t-1}) = p_{22}. \tag{4}$$

Thus, the transition matrix $P(t)$ can be written as follows:

$$P(t)=\begin{bmatrix} p_{11} & p_{12} \\ p_{21} & p_{22} \end{bmatrix}=\exp(\Theta), \tag{5}$$

where $\Theta=\begin{bmatrix} -\omega_1 & \omega_1 \\ \omega_2 & -\omega_2 \end{bmatrix}$ denotes a transition-rate matrix, and ω_i represents the transition rate leaving from state i to other state j. We denote the joint probability of S_t and N_{t,S_t} as $p_{ij}(m,1)=P(S_{t-1}=i,\ S_t=j, N_{t,S_t}-N_{t-1,S_t}=m)$, which represents the one-period transition probability with m arrival times from state $S_{t-1}=i$ to state $S_t=j$. Last and Brandt (1995) give the moment-generating function for this joint distribution function as follows:

$$P^*(z,1)=\sum_{m=0}^{\infty}\mathrm{P(m,1)}z^m,\ 0<z<1, \tag{6}$$

where $\mathrm{P(m,1)}\equiv(p_{ij}(m,1))$ represents the 2×2 transition probability matrix. The moment-generating function under the Kolmogorov forward equation has a unique solution for $\mathrm{P(m,1)}=\mathrm{e}^{[\Theta-(1-m)\Lambda]}$, where Λ is the weather-induced CAT intensity matrix,

$$\Lambda=\begin{bmatrix} \lambda_{t,1} & 0 \\ 0 & \lambda_{t,2} \end{bmatrix}. \tag{7}$$

and λ_{t,S_t} represents the weather-induced CAT intensity at state $S_t=\{1,2\}$ from time $t-1$ to t.

We extend Elsner et al. (2008) to capture the asymmetric impact of natural climate cycles and global warming on weather-induced CAT intensity by proposing a two-state regime-switching Poisson regression function that includes the AMO and CO_2 as climate variables to model weather-induced CAT intensity. Weather-induced CAT intensity is higher in one state because of the effects of high AMO and CO_2, but it is lower in another state because of the effects of low AMO and CO_2. Therefore, the model of weather-induced CAT intensity at state S_t is as follows:

$$\lambda_{t,S_t} = \begin{cases} \exp(\lambda_1^1 + \lambda_1^2 AMO_t + \lambda_1^3 CO_{2,t}), & \text{in higher CAT events } (S_t = 1) \\ \exp(\lambda_2^1 + \lambda_2^2 AMO_t + \lambda_2^3 CO_{2,t}), & \text{in lower CAT events } (S_t = 2) \end{cases} \quad (8)$$

where $\lambda_{S_t}^1$ describes the state-dependent drift term of intensity from time $t-1$ to time t, $\lambda_{S_t}^2$ represents the state-dependent parameter of the AMO effect on the weather-induced CAT event to capture the impact of the natural climate cycle on CAT intensity and $\lambda_{S_t}^3$ represents the state-dependent parameter of the CO_2 effect on weather-induced CAT event to capture the impact of global warming on CAT intensity.

In predicting the future weather-induced CAT intensity, we model the dynamics of AMO and changes in CO_2 using a standard *ARMA*(*p*, *q*) time series model:

$$I_t = w_t^I + \sum_{i=1}^{p} \alpha_i^I I_{t-i} + \sum_{j=0}^{q} \beta_j^I \varepsilon_{t-j}^I, I = AMO \text{ or } CO_2, \quad (9)$$

where p and q denote the AR and MA orders, respectively; α_i^I and β_j^I are the AR and MA coefficients of the AMO and CO_2, respectively; and setting $\beta_0^I = 1, I = AMO \text{ or } CO_2$. w_t^I is an arbitrary constant, and ε_t^I is independent and normally distributed with a mean of zero and a variance of $\sigma_I^2 > 0$.

We can forecast future AMO and CO_2 with Equation (9). Therefore, Equation (8) can be rewritten using the predicted values of AMO (AMO_t^*) and CO_2 ($CO_{2,t}^*$):

$$\lambda_{t,S_t} = \begin{cases} \exp(\lambda_1^1 + \lambda_1^2 AMO_t^* + \lambda_1^3 CO_{2,t}^*), & \text{in higher CAT events } (S_t = 1) \\ \exp(\lambda_2^1 + \lambda_2^2 AMO_t^* + \lambda_2^3 CO_{2,t}^*), & \text{in lower CAT events } (S_t = 2) \end{cases} \quad (10)$$

where

$$AMO_t^* = (w_t^{AMO} + \sum_{i=1}^{p} \alpha_i^{AMO} AMO_{t-i} + \sum_{j=1}^{q} \beta_j^{AMO} \varepsilon_{t-j}^{AMO}), CO_{2,t}^* = (w_t^{CO_2} + \sum_{i=1}^{p} \alpha_i^{CO_2} CO_{2t-i} + \sum_{j=1}^{q} \beta_j^{CO_2} \varepsilon_{t-j}^{CO_2}).$$

Equation (10) indicates that the intensity of a weather-induced CAT at time t can be obtained from the past information of the AMO index and the CO_2 index in the *ARMA*(*p*, *q*) model. Thus, we are able to predict hurricane intensity and the natural logarithm of the

hurricane intensity contains the mean reverting property. If we do not consider the regime-switching effect and the CO_2 effect, ($\lambda_1^1 = \lambda_2^1, \lambda_1^2 = \lambda_2^2, \lambda_1^3 = \lambda_2^3 = 0$), Equation (10) reduces to the model of Elsner et al. (2008). If $\lambda_{S_t}^2 = \lambda_{S_t}^3 = 0$ (i.e., where there is no AMO effect and no CO_2 effect), Equation (10) reduces to the model of Chang, Lin and Yu (2011). If $\lambda_1^1 = \lambda_2^1$, $\lambda_{S_t}^2 = \lambda_{S_t}^3 = 0$ and there is no regime-switching effect, Equation (10) reduces to the traditional Poisson model.

3. Empirical Analysis

3.1 Preliminary Data Analysis

This section employs the AMO index, the CO_2 index and annual hurricane frequency from 1961 through 2010 for our analyses. The data from the AMO and CO_2 indices are extracted from the National Oceanic and Atmospheric Administration (NOAA), and hurricane frequency and losses are available from the U.S. database on spatial hazard events and losses. The AMO index is computed by averaging SSTs between 0° and 60°N and 75° and 7.5°W. The CO_2 index in the Earth's atmosphere (parts per million) derived from in situ air measurements at the Mauna Loa Observatory, Hawaii: Latitude 19.5Â°N Longitude 155.6Â°W Elevation 3397m. Utilizing data covering the 1961-2010 period, Figures 1 and 2 show the time series relationship among of the AMO index, the CO_2 index and hurricane frequency from 1961 to 2010. The correlation coefficient of the AMO index (CO_2 index) and hurricane frequency is approximately 53% (55%). Thus, the AMO and CO_2 indices are each positively related to hurricane frequency.

[Figure 1 is here]

[Figure 2 is here]

Table 2 provides the descriptive statistics for the AMO index, the CO_2 index and hurricane frequency from 1961 to 2010. The skewness of the AMO and CO_2 indices is close to zero, and the excess kurtosis is also close to zero. We employ standard tools of time-series analysis to assist us in modeling the AMO index and changes in the rate of the CO_2 index. The first step in the development of a time-series model is to check for stationarity. We then use the Phillips-Perron (PP) test (Phillips and Perron, 1988) to investigate the null hypothesis that a time series is non-stationary with a unit root. The PP method estimates the non-augmented Dickey-Fuller test and modifies the t-ratio of the alpha coefficient such that serial correlation does not affect the asymptotic distribution of the test statistic. Finally, we use the Ljung-Box (LB) test and Jarqur-Bera (JB) test to check for normality.

[Table 2 is here]

Table 3 reports the results of the unit root tests for the AMO index, the CO_2 index and the change rate of CO_2 index. The PP tests reject the null hypothesis of the unit root for the AMO index and for the change rate of CO_2 index, but the CO_2 index fails to reject the null hypothesis of the unit root. Consequently, we use the AMO index and the change rate of CO_2 index in further analyses.

[Table 3 is here]

We use univariate autoregressive moving average (ARMA) models for hurricane intensity projection. We employ data from the 1961 to 2010 period and determine that the ARMA(1,1) is the optimal model for the AMO index and the change rate of CO_2 index (ΔCO_2) based on the Akaike information criterion (AIC) and the Schwarz Bayesian information criterion (BIC) values. The estimated result is the following:

$$\underset{(0.0861)***}{AMO_t = 0.9221 AMO_{t-1}} + \varepsilon_t^{AMO} \underset{(0.2041)**}{- 0.4150 \varepsilon_{t-1}^{AMO}}, \ \varepsilon_t^{AMO} \sim N(0, 0.0166),$$

$$\Delta CO_{2,t} = \underset{(0.0117)***}{0.9999}\Delta CO_{2,t-1} + \varepsilon_t^{\Delta CO_2} - \underset{(0.0974)***}{0.8259}\varepsilon_{t-1}^{\Delta CO_2},\ \varepsilon_t^{\Delta CO_2} \sim N(0, 2.076*10^{-6}) \quad (11)$$

The LB and JB tests show that the LB and JB statistics for the residuals of the AMO index (the change rate of CO_2 index) are 11.6696 (15.079) and 4.6417 (2.7209), respectively, which is not statistically significant at the 5% level. Therefore, we can say that ARMA(1,1) is appropriate model for the AMO index and the change of CO_2 index.

3.2 Parameter Estimation for Hurricane Risk

Table 4 reports the estimates of hurricane intensity using linear and regime-switching models after obtaining the coefficient estimates for the parameters of the AMO and the change rate of CO_2 indices from Equation (11). Table 4 shows the goodness-of-fit of hurricane intensity for four linear models, including the linear constant model (LM), the linear model with AMO index (LAM), the linear model with CO_2 index (LCM) and the linear model with both AMO and CO_2 indices (LACM), in addition to four regime-switching models, including the regime-switching constant model (RM), the regime-switching model with AMO index (RAM), the regime-switching model with CO_2 index (RCM) and the RACM. The coefficient of the constant term, λ_1^1=1.5173, in the LM corresponds to the mean value of hurricane frequency (λ_t) of 4.560 reported in Table 2. However, its significance is only at 12.92% level. The LAM model finds that the coefficient of the AMO index, $\lambda_1^2 = 4.3723$, is significant at the 1% level, which implies that hurricane intensity is significantly and positively affected by the AMO index, which is consistent with the empirical evidence of Elsner et al. (2008). We further consider the impact of global warming on hurricane intensity. The coefficient of the CO_2 index, $\lambda_1^3 = 495.9430$, in the LCM is significant at the 1% level, which indicates that hurricane intensity is significantly and positively affected by the CO_2 index. This result implies that the CO_2 index also influences hurricane intensity, which is supported by the IPCC report (2007) and indicated that future climate change may become more serious as a result of human-induced global warming and may increase unanticipated hurricane events. The LAM and LCM models produce a better fit than the LM model based on the AIC and the BIC values. This result demonstrates that the AMO index and the CO_2 index must be considered in analyzing and predicting hurricane intensity.

[Table 4 is here]

Table 4 shows the goodness of fit of hurricane intensity for four regime-switching models. The results reveal that the coefficient of the AMO index in the high regime is significantly positive at the 1% level ($\lambda_1^2 = 4.1638$), and the corresponding coefficient in the low regime is significant at the 10% level ($\lambda_2^2 = 0.5726$) in the RAM. The RCM demonstrates that the coefficient of the CO_2 index in the high regime is significantly positive at the 1% level ($\lambda_1^3 = 157.6834$), but the corresponding coefficient of the AMO index in the low regime is not significant ($\lambda_2^3 = 0.0006$). These results imply that the CO_2 index exerts an asymmetric effect on hurricane intensity. The effect of the CO_2 index on hurricane intensity would increase in the high regime. By contrast, the significant influence of the CO_2 index vanishes in the low regime. Furthermore, increased hurricane intensity is driven by the higher AMO index and the CO_2 index in the high regime. We also observe that the regime-switching models dominate the linear models, and RACM offers the best fit for the hurricane intensity based on the AIC and the BIC values. The transition probabilities, p_{11} and p_{22}, are 0.7382 and 0.2685, respectively. These results imply that the probability of switching from low hurricane intensity to high hurricane intensity is higher than switching from high hurricane intensity to low hurricane intensity.

We further use the maximum likelihood estimation to estimate the parameter values of losses caused by hurricanes using several popular distributions. The empirical results are shown in Table 5. We find that the gamma distribution exhibits the best goodness-of-fit with an estimated shape parameter of $\alpha = 0.134$ and scale parameter $\beta = 0.152$, which are significant at the 1% and 5% levels, respectively. Its value of the log-likelihood function is 327.625.

[Table 5 is here]

3.3 Prediction of Hurricane Intensity

The empirical results from the previous section provide us with the background to develop a prediction algorithm for hurricane intensity. Specifically, we use the ARMA(1,1) model in Equation (11) to predict future AMO/CO_2 index and use then compute the corresponding hurricane intensity. Taking the ARMA(1,1) model of the AMO/CO_2 index as an example, we obtain a predicted AMO/CO_2 index for the 2007-2010 periods by using the historical AMO/CO_2 index for the 1961-2006 periods. Finally, based on the predicted AMO/CO_2 index, each model produces the corresponding hurricane intensity from 2007 to 2008, 2008 to 2009 and 2009 to 2010. We employed the mean absolute error (MAE) and the root mean square error (RMSE) methods to measure projection performance and the predictive power of the models.

Table 6 reports the prediction errors of annual hurricane intensity given the actual AMO/CO_2 index and the predicted AMO/CO_2 index using the ARMA(1,1) model. The MAE and the RMSE find that LAM (LACM) produces better prediction performance than LM (LAM), which suggests that the effects from both the AMO and CO_2 should be considered. Furthermore, we find that the RACM produces better prediction performance than the LACM with an improvement rate about 60% (i.e. (2.7496-1.1050)/ 2.7496; see Table 6, Panel A).

Panel B shows that employing the predicted AMO and CO_2 indices from ARMA(1,1) model produces the lowest forecasting errors in RACM. This finding implies that the regime-switching Poisson regression using the predicted AMO and CO_2 values provides a better means of predicting U.S. hurricane frequency. The minimum MAE of this model is only 1.0848 which is low comparing with our sample mean of 4.56 hurricane events per year. This indicates that our forecasting error for the annual U.S. hurricane frequency is about one.

[Table 6 is here]

4. Applications: Risk Management and Valuation of CAT Reinsurance

4.1 Hurricane Risk Measurements: TailVaR

Several measures of tail risk are used for to measure CAT risk. The best known measure is "value at risk" (VaR), which is the quantile of the loss distribution at a remote return period. However, the VaR measure ignores the shape of the risk in the tail of the distribution. A more common measure adopted by reinsurers is expected shortfall or TailVaR. TailVaR measures the expected loss after the loss exceeds a given remote threshold. This section measures the TailVaR of hurricane risk from 2007 to 2010 based on the four models (the LM, LAM, LACM, and RACM). We then investigate the influence of the regime-switching effect, the AMO effect and the CO_2 effect on the TailVaR for reinsurers with hurricane risk.

The value of TailVaR is obtained as follows:

1. We first compute the hurricane loss of a specific event using the RSCP model because hurricane loss of each event and hurricane frequency are independent. Based on the hurricane loss data from 1961 to 2006, it shows that the gamma distribution exhibits the best goodness-of-fit with an estimate of a shape parameter of $\alpha = 0.129$ and a scale parameter $\beta = 0.168$. Therefore, we simulate 100,000 paths for the gamma random variables using the shape parameter $\alpha = 0.129$ and the scale parameter $\beta = 0.168$ to generate specific hurricane loss for each event from 2007 to 2010.
2. We simulate 100,000 paths using the standard normal random variables to generate the AMO index and changes in the CO_2 index using ARMA(1,1) from 2007 to 2010, which allows us to compute hurricane intensity with the RACM, the LACM and the LAM in each year.
3. We compute the expected value for the 1,000 extreme paths of total hurricane losses to obtain the TailVaR of hurricane risk based on the RACM, LACM, LAM and LM

in each year at the 1% significance level.

Figure 3 presents the TailVaR estimated from our four CAT intensity models. This figure shows that the TailVaR in LM is much lower than those from the LAM, LACM and RACM. The differences show that AMO effect is larger than the CO_2 effect and the regime-switching effect is substantial in all four years. In particular, Hurricane Ike alone caused a $12.5 billion insured loss in September 2008, while the LM produces a TailVaR of less 2 billion (1.79 billion) in the year of 2008. However, the RACM suggests a TailVaR of 13.39 billion which seems to be a more reasonable reserve for the insurance industry to cover the hurricane risk.

[Figure 3 is here]

We further compare the RACM, LACM, LAM and LM to obtain greater insight on the influence of the regime-switching effect, the CO_2 effect and the AMO effect on TailVaR. We consider the LM as the benchmark and define the changes of TailVaR as follows:

$$\text{Let } \triangle \text{TailVaR} \equiv \text{TailVaR(RACM)} - \text{TailVaR(LM)}$$

$$= [\text{TailVaR(RACM)} - \text{TailVaR(LACM)}] + [\text{TailVaR(LACM)} - \text{TailVaR(LAM)}] + [\text{TailVaR(LAM)} - \text{TailVaR(LM)}]$$

$$= \triangle \text{TailVaR resulting from the regime-switching effect} + \triangle \text{TailVaR resulting from the } CO_2 \text{ effect} + \triangle \text{TailVaR resulting from AMO effect}$$

$$\equiv \text{Regime-switching effect} + CO_2 \text{ effect} + \text{AMO effect}$$

$$\equiv \text{Total effect} \qquad (12)$$

We use Equation (12) to compute the total effect, the regime-switching effect, the CO_2 effect and the AMO effect; the results are shown in Figure 4. Figure 4 indicates that the regime-switching effect and the AMO effect dominate the CO_2 effect in each year and that the CO_2 effect is the largest in 2008. This result indicates the importance of incorporating the regime-switching effect, the CO_2 effect and the AMO effect in managing hurricane risk and forecasting hurricane activity.

[Figure 4 is here]

4.2 Valuation of stop-loss reinsurance

This section illustrates the payoff of a stop-loss CAT reinsurance contract and uses the discrete-time Esscher transformation to price the reinsurance via the equivalent martingale probability measure. The aggregate CAT loss is assumed to follow the regime-switching compound process (RSCP).

The stop-loss reinsurance contract offers a protection for losses exceeding M and the protection is capped at C. By design, if the aggregate CAT loss, Y_{T,S_t}, is less than the protection M, the reinsurer pays nothing. However, when the aggregate CAT loss, Y_{T,S_t}, exceeds the protection M, reinsurance pays $Y_{T,S_t} - M$ up to the limit of the reinsurer's exposure, $C - M$. The payoff of the reinsurer for the contract at maturity T, $V(T)$, is:

$$V(T) = \min(\max(Y_{T,S_t} - M, 0), C - M) = \max(Y_{T,S_t} - M, 0) - \max(Y_{T,S_t} - C, 0). \qquad (13)$$

Thus the stop-loss reinsurance is simply the difference between two call options with different strike prices (*M* and *C*) that are written on the same underlying losses.

Change measure: discrete-time Esscher transform

When the market is incomplete, there are infinitely many equivalent martingale measures. The Esscher transform is a well-known tool in actuarial science and finance. Its history may be tracked to the seminal work of Esscher (1932), in which this transform was first introduced to the actuarial science literature. The original purpose of the Esscher transform was to provide a convenient method to approximate the distribution of aggregate claims. Gerber and Shiu (1994) adopt the continuous-time Esscher transform to price options embedded in insurance products in an incomplete market. The Esscher transform has the advantage that the dynamic structure of invariance can be maintained after a measure transform. The existence condition of the moment-generating function remains qualified

regardless of the size of CAT events. Furthermore, the Esscher transform can be regarded as the general Girsanov transformation. Elliott et al. (2005) provide the continuous-time regime-switching version of the Esscher transform to determine an equivalent martingale measure. Christoffersen et al. (2010) employ the discrete-time Esscher transform to determine an equivalent martingale measure in an incomplete market. Since both the AMO and CO_2 indices are discrete, we thus follow Christoffersen et al. (2010) in the following analysis.

We use P to describe the physical distribution of the states of nature. We assume that a finite time t is specified by $[0,1,2,...,T]$ and that the financial market consists of a zero-coupon risk-free bond index and a CAT claim. The dynamics of the bond are described by the process $\{B_t\}_{t=0}^{T}$ normalized to $B_0 = 1$. The dynamics of the aggregate CAT losses of CAT events are described by $\{Y_t\}_{t=0}^{T}$. The information structure is given by the filtration $\mathrm{F}=\{F_t | t = 0,1,...,T\}$ generated by the CAT claim and the bond process. We follow Elliott et al. (2005) to assume the information of the transition of the state $\{S_t\}_{t=0}^{T}, F_t^{S_t}$, is known in the future; there is no risk premium when the state changes into another state. We follow Christoffersen et al. (2010) to do not constrain the interest rate r_t at time t to be constant; instead, it is assumed to be $F_{t-1}^{r_t}$ measureable. Specifically, the discrete-time Esscher transform is given in the following equation,

$$\left.\frac{dQ}{dP}\right|_{F_t} = \prod_{i=1}^{t}\left[\frac{\exp(h_i Y_i)}{E_{t-1}^{P}\left[\exp(h_i Y_i)\right]}\right] = \exp\left(\sum_{i=1}^{t}(h_i Y_i - \Psi_i(h_i))\right), \tag{14}$$

where h_t denotes the time-varying parameter of the discrete-time Esscher transform, and $\Psi_t(h_t)$ is defined as the natural logarithm of the moment-generating function for the total loss, i.e., $\exp[\Psi_t(h_t)] \equiv E_{t-1}^{P}(\exp(h_t Y_t))$.

According to the definition of a martingale condition on $F_t^{S_t}$ for the discounted aggregate CAT loss under the risk-neutral measure, $E_{t-1}^{Q}\left[Y_t/B_t\right]=Y_{t-1}/B_{t-1}$, the martingale condition holds if and only if the parameters of the Esscher transform h_t satisfy the following:

$$E_{t-1}^{P}\left(Y_t\exp(h_tY_t)\right)\exp(-r_t)-Y_{t-1}\exp(-\lambda_{t,S_t}(\phi_t(h_t)-1))=0 \tag{15}$$

where $E_{t-1}^{P}\left(Y_t\exp(h_tY_t)\right)$ can be obtained by the MATLAB command for a Taylor polynomial. Term $\phi_t(h_t)\equiv E_{t-1}^{P}\left(\exp(h_ty_t)\right)$ is the moment-generating function for the specific loss y_t.

The solution of the martingale condition reveals that the dynamic of the RSCP model by the discrete-time Esscher transform under the risk-neutral probability measure Q, which can be shown as follows and the detailed proof in Appendix A,

$$Y_t^Q=\begin{cases}\sum_{n=N_{t-1,1}^Q}^{N_{t,1}^Q} y_n^Q=Y_{t,1}^Q & if \quad S_t=1,\\ \sum_{n=N_{t-1,2}^Q}^{N_{t,2}^Q} y_n^Q=Y_{t,2}^Q & if \quad S_t=2,\end{cases}$$

where N_{t,S_t}^{Q} denotes a new regime-switching Poisson process with a new intensity matrix Λ^Q of weather-induced events, as follows:

$$\Lambda^Q=\begin{bmatrix}\lambda_{t,1}\phi_t(h_t) & 0\\ 0 & \lambda_{t,2}\phi_t(h_t)\end{bmatrix}, \tag{16}$$

where the invariant Markov chain S_t has an original matrix of the transition rate Θ that remains unchanged under the risk-neutral probability measure. Based on the new intensity matrix and the invariant Markov chain S_t, the one-period joint probability under the risk-neutral probability measure is defined by $Q_{ij}(m,1)=Q(S_{t-1}=i,\ S_t=j,\ N_{t,S_t}-N_{t-1,S_t}=m)$, and the joint probability under the risk-neutral measure can be determined from the

moment-generating function, $Q(m,1) = e^{[\Theta-(1-m)\Lambda^Q]}$. Finally, under the risk-neutral probability measure Q, the new density function of each specific weather-induced CAT loss is:

$$f^Q(y_t) = \frac{e^{h_t y_t}}{\phi_t(h_t)} f(y_t), \tag{17}$$

where $f(y_t)$ is the original density function of each specific weather-induced CAT loss. Many distributions, such as gamma, lognormal and Pareto, can also be applied for claim size distribution. In Table 5, we have shown that gamma distribution fits best for the U.S. hurricane losses during the period of 1961 to 2010.

Closed-form solutions of reinsurance premium

If the stop-loss reinsurance has a maturity of T years, and the claim is settled at each year, the value of the reinsurance at time 0, or reinsurance premium, is

$$V(0) = \sum_{t=1}^{T} e^{-r_t} E_{t-1}^{Q}\left[(Y_{t,S_t} - Y_{t-1,S_t} - M)^+ - (Y_{t,S_t} - Y_{t-1,S_t} - C)^+ \right], S_t = \{1,2\}, \tag{18}$$

where Y_{t,S_t} denotes the aggregate CAT loss at state S_t during t years. The formula of the reinsurance premium can be obtained as Theorem 1.

Theorem 1: Based on the RSCP model, the closed-form solution of the stop-loss reinsurance premium under the risk-neutral probability measure Q is as follows:

$$V(0) = \sum_{t=1}^{T} e^{-r_t} \sum_{m=0}^{\infty} \sum_{i}^{2} \sum_{j}^{2} \pi_i Q_{ij}(m,1) \left[\int_M^{\infty} (y_{t,j}^m - M) f^Q(y_t^m) dy_t^m - \int_C^{\infty} (y_t^m - C) f^Q(y_t^m) dy_t^m \right], \tag{19}$$

where $\pi_1 = \frac{\omega_2}{\omega_1 + \omega_2}, \pi_2 = 1 - \pi_1$ and $Q_{ij}(m,1)$ represents the transition probability with m arrival times from state $S_{t-1} = i$ to state $S_t = j$, in which the hurricane intensity is

$\lambda_{t,i}^{Q} = e^{\lambda_i^1 + \lambda_i^2 AMO_t^* + \lambda_i^3 CO_{2,t}^*} (1 - \frac{h_t}{\beta})^{\alpha}$. $\int_k^{\infty} (y_t^m - k) f^Q(y_t^m) dy_t^m = \frac{\alpha m}{(\beta - h_t)} \left(1 - \frac{\gamma(\alpha m + 1, (\beta - h_t)k)}{\Gamma(\alpha m + 1)} \right)$

$-k\left(1 - \frac{\gamma(\alpha m, (\beta - h_t)k)}{\Gamma(\alpha m)} \right)$, $k = C \text{ or } M$, and γ is the lower incomplete gamma functions.

Equation (19) can be viewed as the sum of transition probability of the difference between two call options with different strike prices (*M* and *C*). Appendix B provides the proof.

We consider several special cases to further illustrate the property of the stop-loss reinsurance solution and to show their specific formulae in the following remarks.

Remark 1: If $Y_t^Q = \sum_{n=N_{t-1,S_t}^Q}^{N_{t,S_t}^Q} y_n^Q$, where N_{t,S_t}^Q is a regime-switching Poisson process and the hurricane intensity is constant at different states (i.e., no AMO effect and no CO_2 effect ; $\lambda_{S_t}^2 = \lambda_{S_t}^3 = 0$), the hurricane intensity will reduce to the model in Chang et al. (2011), and the pricing formula for the stop-loss reinsurance can be derived as the following:

$$V(0) = \sum_{t=1}^{T} e^{-r_t} \sum_{m=0}^{\infty} \sum_{i}^{2} \sum_{j}^{2} \pi_i \, Q_{ij}(m,1) \left[\int_M^{\infty} (y_t^m - M) f^Q(y_t^m) dy_t^m - \int_C^{\infty} (y_t^m - C) f^Q(y_t^m) dy_t^m \right],$$

where $Q_{ij}(m,1)$ represents the transition probability with m arrival times from state $S_{t-1} = i$ to state $S_t = j$ and its hurricane intensity is $\lambda_{t,S_t}^Q = \mathrm{e}^{\lambda_i^1}(1 - \frac{h_t}{\beta})^{\alpha}$.

Remark 2: If $Y_t^Q = \sum_{n=N_{t-1}^Q}^{N_t^Q} y_n^Q$, where N_t^Q is the Poisson process, and the hurricane intensity is a linear function of the AMO index and the CO_2 index $(\lambda_1^1 = \lambda_2^1, \lambda_1^2 = \lambda_2^2, \lambda_1^3 = \lambda_2^3)$, the pricing formula for the stop-loss reinsurance is as follows:

$$V(0) = \sum_{t=1}^{T} e^{-r_t} \sum_{m=0}^{\infty} \frac{e^{-\lambda_t^Q} (\lambda_t^Q)^m}{m!} \left[\int_M^{\infty} (y_t^m - M) f^Q(y_t^m) dy_t^m - \int_C^{\infty} (y_t^m - C) f^Q(y_t^m) dy_t^m \right],$$

where $\lambda_t^Q = \mathrm{e}^{\lambda_t^1 + \lambda_t^2 AMO_t^* + \lambda_t^3 CO_{2,t}^*}(1 - \frac{h_t}{\beta})^{\alpha}$.

If the hurricane intensity is only a linear function of the AMO index $(\lambda_1^1 = \lambda_2^1,\ \lambda_1^2 = \lambda_2^2,\ \lambda_1^3 = \lambda_2^3 = 0)$, the hurricane intensity reduces to the model in Elsner et al. (2008), and the hurricane intensity under the risk-neutral world becomes

$\lambda_t^Q = \mathrm{e}^{\lambda_t^1 + \lambda_t^2 AMO_t^*}(1-\frac{h_t}{\beta})^{\alpha}$. If the hurricane intensity is only a linear function of the CO_2 index $(\lambda_1^1 = \lambda_2^1,\ \lambda_1^2 = \lambda_2^2 = 0,\ \lambda_1^3 = \lambda_2^3)$, the hurricane intensity under the risk-neutral world becomes $\lambda_t^Q = \mathrm{e}^{\lambda_t^1 + \lambda_t^3 CO_{2t}^*}(1-\frac{h_t}{\beta})^{\alpha}$. If the hurricane intensity at different states is constant and the same $(\lambda_1^1 = \lambda_2^1 = \lambda_1^2 = \lambda_2^2 = \lambda_1^3 = \lambda_2^3 = 0)$, the hurricane intensity reduces to the traditional Poisson model and the hurricane intensity under the risk-neutral world becomes $\lambda_{t,S_t}^Q = \mathrm{e}^{\lambda_i^1}(1-\frac{h_t}{\beta})^{\alpha}$.

4.3 Numerical Analysis

This section evaluates the pricing performance for the stop-loss CAT reinsurance using the four alternative hurricane intensity models: RACM, LACM, LAM, and LM. We also look into the effect of the regime-switching effects, the AMO effect and the CO_2 effect, on the reinsurance premium.

Parameter values

We assume the following parameter values for the stop-loss reinsurance: protection, $M = 1$; cap, $C = 5$; interest rate, $r_t = 0.02$; and the reinsurance maturity, $T = 1$. Furthermore, the hurricane intensity, λ_{t,S_t}^Q, of the different models in the risk-neutral world can be obtained according to the estimated parameter values ($\lambda_{S_t}^1, \lambda_{S_t}^2, \lambda_{S_t}^3$) of RACM, LACM, LAM and LM, the h_t value implied by Equation (15), and the shape (scale) parameter value α (β) for the gamma distribution during 1961-2006 period. The transition probability at hurricane frequencies from state 1 to state 2 is $p_{12} = 0.1781$ and $p_{11} = 0.8219$, respectively, for the RACM. Consequently, the probability from state 2 to state 1 is $p_{21} = 0.7484$ and $p_{22} = 0.2516$ respectively. Using the transition probability, the transition rate of two states can be obtained ($\omega_1 = 0.5018$, and $\omega_2 = 2.1087$) to capture the leaving length of intensity at a different state.

To compute the sequence of transition probability under the risk-neutral world,

$\{Q(m,1),m>0\}$, we adopt the method proposed by Abate and Whitt (1992), who present a simple algorithm for numerically inverting probability-generating functions based on the Fourier series method to obtain a simple computation with a convenient error bound from the discrete Poisson summation formula. Let $i=\sqrt{-1}$, and let $\mathrm{Re}(z)$ be the real part of z. For $0<\varepsilon<1$ and $m\geq 1$,

$$\left|Q(m,1)-\tilde{Q}(m,1)\right|\leq \frac{\varepsilon^{2m}}{1-\varepsilon^{2m}},$$

where $$\tilde{Q}(m,1)=\frac{1}{2m\varepsilon^{m}}\left[Q^{*}(\varepsilon,1)+(-1)^{m}Q^{*}(-\varepsilon,1)+2\sum_{k=1}^{m-1}(-1)^{k}\,\mathrm{Re}(Q^{*}(\varepsilon\exp(\frac{\pi ki}{m}),1))\right],$$

$Q^{*}(z,1)=\sum_{m=0}^{\infty}Q(m,1)z^{m}$, $0<z<1$. Note that the infinite summation of hurricane events, *m*, is truncated at level *m* = 20 such that the respective cumulative Poisson probabilities are very close to 1.

Scenario Analysis

We conduct a scenario analysis to examine the regime-switching effect, the AMO effect and the CO_2 effect on the value of reinsurance from 2007 to 2009. Table 7 shows the scenario analysis of annual hurricane intensity using the different models from 2007 to 2009. Panels A and B indicate that the value of reinsurance in the LM, LAM, LCM and LACM are underestimated, particularly in the LM. Furthermore, the value of reinsurance in the RACM is the largest in 2007 because Hurricane Ike occurs and causes 12.5 billion in insured losses in September 2008. Thus, the discounted hurricane loss value and the reinsurance premium are highest in that year. However, the stop-loss premium in the LM in 2007 is underestimated and fails to capture and forecast future hurricane intensity. This result indicates that the regime-switching effect, the CO_2 effect and the AMO effect must be considered when pricing weather-induced CAT products.

[Table 7 is here]

Measurement Errors

We obtain the real value (V_R) of the reinsurance using the actual frequency and loss data of hurricane events, and the theoretical value (V_T) of the reinsurance using estimated parameter values from the RACM, LACM, LCM, LAM and LM in 2007, 2008 and 2009. We compute two measurements of pricing errors, the MAE and RMSE methods, for purposes of comparison.

Table 8 provides an overview of the MAE and RMSE measurements of pricing errors. Panels A and B indicate that the pricing errors under the RACM are all smaller than the errors under the LM, LAM, LCM and LACM for the MAE and RMSE measurements. Using the MAE in Panel B as an example, the improvement rate of pricing errors using the LCM over the LM is only 29.93 percent [(1.4815−1.0380)/1.4815]. The improvement rate rises to 43.41 (41.33) percent if we use the LAM (LACM). Furthermore, the improvement rate increases to 68.40 percent [(1.4815−0.4682)/1.4815] if the hurricane activity is assumed to follow the RACM. Our results show that the RACM can reduce pricing errors by 55–70 percent depending on the MAE and RMSE measurement methods.

[Table 8 is here]

5. Conclusions

This paper develops a regime-switching compound Poisson (RSCP) model in which the two-state hurricane intensity is a function of a natural climate cycle (AMO index) and global warming (CO_2 index), to forecast weather-induced CAT intensity and price CAT risk. With respect to the regime-switching model, the empirical results indicate that the effect of the AMO index and the CO_2 index on the frequency of hurricane events would increase in the high regime. This result can be explained by the IPCC report (2007), which indicates that future climate change may become more serious as a result of human-induced global warming and lead to more unanticipated hurricane events. By contrast, the significant

influence of the AMO index and/or the CO_2 index vanishes in the low regime. Consequently, we observe an asymmetric effect of the AMO index on hurricane intensity, and the CO_2 index affects the hurricane intensity in the high regime. The empirical results of the regime-switching model that considers the AMO index and the CO_2 effect provide an excellent projection average annual U.S. hurricane frequency, with a forecasting error of about one.

With respect to hurricane risk management using TailVaR and the pricing of stop-loss reinsurance, we find that insurers can provide the appropriate reserves to manage hurricane risk by using the regime-switching model that considers the AMO index and the CO_2 effect. Furthermore, pricing errors related to stop-loss premiums under the RACM are 55 to 70 percent less than under the LCM. The regime-switching effect and the AMO effect dominate the CO_2 effect, and the CO_2 effect is the largest in 2008 during Hurricane Ike. This result indicates the importance of considering the regime-switching effect, the CO_2 effect and the AMO effect when managing hurricane risk, when modeling and forecasting hurricane activity and when pricing weather-induced CAT products.

Table 1: Ten Most Costly Catastrophes in the United States.

Rank	Month/Year	Event	Estimated Insured Losses	
			Dollars when Occurred	In 2012 Dollars ($ Billions)
1	Aug. 2005	Hurricane Katrina	$41.100	$48.317
2	Sep. 2001	World Trade Center & Pentagon Terrorist Attacks	$18.779	$24.345
3	Oct. 2012	Hurricane Sandy	$18.750	$18.750
4	Aug. 1992	Hurricane Andrew	$15.500	$25.364
5	Jan. 1994	Northridge, CA Earthquake	$12.500	$19.365
6	Sept. 2008	Hurricane Ike	$12.500	$13.329
7	Oct. 2005	Hurricane Wilma	$10.300	$12.108
8	Aug. 2004	Hurricane Charley	$ 7.475	$ 9.085
9	Apr. 2011	Flooding and tornados that struck Tuscaloosa, AL, & other locations	$ 7.300	$ 7.451
10	Sep. 2004	Hurricane Ivan	$ 7.110	$ 8.641

Sources: Insurance Services Office, Inc. (ISO), 2013.

Table 2: Descriptive Statistics of Hurricanes and Climate Variables from 1961 to 2010.

	Frequency	AMO	CO_2	Change rate of CO_2
Mean	4.560	-0.04	348.581	0.004
Median	3	-0.061	346.713	0.004
Min	0	-0.061	317.638	0.001
Max	18	0.383	389.845	0.008
Std. Dev.	4.550	0.193	21.795	0.002
Skewness	1.300	0.249	0.268	0.199
Excess Kurtosis	0.788	-0.46	-1.136	-0.280

Table 3: Phillips-Perron Unit Root Tests.

	Intercept	Trend & Intercept	None
AMO index	-2.36**	-2.34	-3.73**
CO_2 index	19.58	5.49	-1.28
Change rate of CO_2	-1.11	-4.92***	-6.54***

Asterisks denote statistical significance at the 1% (***) and 5% (**) levels.

Table 4: Parameter Estimates of U.S. Hurricane Intensity in Linear and Regime-switching Models from 1961 to 2010.

Model	λ_1^1	λ_2^1	λ_1^2	λ_2^2	λ_1^3	λ_2^3	p_{11}	p_{22}	AIC	BIC
LM	1.5173 (0.1292)	--	--	--	--	--	--	--	-307.5082	-305.5962
RM	2.3716 (0.8674)	0.7267 (0.9509)	--	--	--	--	1.0000 (0.976)	0.9888 (0.990)	-404.8736	-397.2255
LAM	1.3778 (0.8742)	---	4.3723*** (0.0057)	--	--	--	--	--	-414.3437	-410.5197
RAM	1.5596 (0.8358)	0.5346 (0.8614)	4.1638*** (0.0028)	0.5726* (0.0944)	--	--	0.7786* (0.0929)	0.2257* (0.0923)	-415.1772	-411.7051
LCM	-0.8222 (0.9143)	--	--	--	495.9430*** (0.0000)	--	--	--	-400.1796	-396.3556
RCM	1.5849 (0.8594)	0.6721 (0.9264)	--	--	157.6834*** (0.0000)	0.0006 (0.9884)	1.0000 (0.088)	0.9872 (0.996)	-404.3732	-400.9010
LACM	1.3987 (0.9521)	--	4.3818* (0.0658)	--	-5.1481*** (0.0000)	--	--	--	-412.3445	-406.6084
RACM	1.3496 (0.8305)	1.1381 (0.8046)	3.7378* (0.0615)	1.0650 (0.8046)	110.4862*** (0.0000)	-198.0596*** (0.0000)	0.7384* (0.094)	0.2685* (0.0976)	-416.1342	-411.8380

The p values are reported in parentheses. Asterisks denote statistical significance at the 1% (***), 5% (**) and 10% (*) levels.

Table 5: Parameter Estimates of Distributions for Hurricane Losses (y) from 1961 to 2010

(Unit: billion)

Distribution		Parameters	Log-likelihood Values
Lognormal	$f\left(y\middle\vert \mu_y,\sigma_y\right)=\frac{1}{y\sigma_y\sqrt{2\pi}}e^{\frac{-(\ln y-\mu_y)^2}{2\sigma_y^2}}$	$\mu_y=-9.678***$ $\sigma_y=11.291***$	292.266
Gamma	$f\left(y\middle\vert \alpha,\beta\right)=\frac{1}{\beta^\alpha\,\Gamma(\alpha)}y^{\alpha-1}e^{\frac{-y}{\beta}}$ where $\Gamma(\alpha)$ is Gamma function	$\alpha=0.134***$ $\beta=0.152**$	327.625
Exponential	$f\left(y\middle\vert \mu_y\right)=\frac{1}{\mu_y}e^{\frac{-y}{\mu_y}}$	$\mu_y=0.021***$	144.350
Weibull	$f\left(y\middle\vert a,b\right)=\frac{b}{a}\left(\frac{y}{a}\right)^{b-1}e^{-(y/a)^b}$	$a=0.002$ $b=0.206***$	316.970
Pareto	$f\left(y\middle\vert k,\sigma\right)=\frac{1}{\sigma}\left(\frac{ky}{\sigma}\right)^{-1-1/k}$	$k=5.124***$ $\sigma=0.0001$	205.871

Asterisks denote statistical significance at the 5% (**) and 1% (***) levels.

Table 6: Prediction Errors of U.S. Annual Hurricane Intensity from 2007 to 2010.

Model	**Panel A Prediction Using Actual AMO and ΔCO_2**		**Panel B Prediction Using ARMA(1,1) for AMO and ΔCO_2**	
	MAE	RMSE	MAE	RMSE
LM	6.6606	6.6802	6.6606	6.6802
RM	4.8852	5.2465	4.8852	5.2465
LAM	1.7966	2.0912	1.4096	1.7027
RAM	1.5561	1.9161	1.2568	1.5581
LCM	3.3291	3.3388	3.5181	3.5418
RCM	2.9263	2.7826	2.9365	2.8936
LACM	2.7496	2.9484	2.7076	2.9209
RACM	1.1050	1.2137	1.0848	1.2056

The table uses mean absolute error (MAE) and the root mean square error (RMSE) methods to measure projection performance and the predictive power of the models. The parameter values for loss distribution are: $\alpha=0.129$, $\beta=0.168$. The parameters of the LM are: $\lambda_1^1=1.3808$. The parameters of the RM are: $\lambda_1^1=2.2535$, $\lambda_2^1=0.7010$. The parameters of the LAM are: $\lambda_1^1=1.3506$, $\lambda_1^2=4.1807$. The parameters of the RAM are: $\lambda_1^1=1.4567$, $\lambda_2^1=0.3788$, $\lambda_1^2=4.1216$, $\lambda_2^2=0.0001$. The parameters of the LCM are: $\lambda_1^1=$-0.7233, $\lambda_1^3=461.4121$. The parameters of the RCM are: $\lambda_1^1=1.898$, $\lambda_2^1=-0.713$, $\lambda_1^3=417.5441$,, $\lambda_2^3=96.2332$.. The parameters of the LACM are: $\lambda_1^1=1.5459$, $\lambda_1^2=4.2393$, $\lambda_1^3=$-5.4527. The parameters of the RACM are: $\lambda_1^1=1.6618$, $\lambda_2^1=1.5884$, $\lambda_1^2=3.9215$, $\lambda_2^2=1.0818$, $\lambda_1^3=1.1141$, $\lambda_2^3=$-243.8173, $\omega_1=0.5018$, $\omega_2=2.1087$, $p_{11}=0.8219$, $p_{22}=0.2516$.

Table 7: Scenario Analysis of the Regime-Switching Effect, AMO Effect and CO2 Effect on Reinsurance Premiums from 2007 to 2009.

Model	Panel A Reinsurance Premiums using Actual AMO and ΔCO_2			Panel B Reinsurance Premiums using ARMA (1,1) for AMO and ΔCO_2		
	2007	2008	2009	2007	2008	2009
LM	2.1203	2.1959	2.1198	2.1203	2.1959	2.1198
LAM	3.3113	2.5536	2.8629	3.5250	3.3285	2.7934
LCM	2.2722	2.2420	3.7300	2.6402	2.6254	2.5007
LACM	3.2519	2.4993	3.4281	3.4333	3.2380	2.6998
RACM	4.1001	3.8693	3.8255	4.1565	4.1033	3.9563

The parameter values for base valuation are: $M=1,\ C=5,\ r_t=0.02,\ T=1,\ m=20,\ \alpha=0.129,\ \beta=0.168$. The parameters of the LM are: $\lambda_1^1=1.3808.\ h_{2007}=$ -0.0937, $h_{2008}=$ -0.0874, $h_{2009}=$ -0.0937. The parameters of the LAM are: $\lambda_1^1=1.3506,\ \lambda_1^2=4.1807,\ h_{2007}=$ -0.0755, $h_{2008}=$ -0.0849, $h_{2009}=$ -0.0437. The parameters of the LCM are: $\lambda_1^1=$ -0.7233, $\lambda_1^3=461.4121,,\ h_{2007}=$ -0.0933, $h_{2008}=$ -0.0884, $h_{2009}=$ -0.0649. The parameters of the LACM are: $\lambda_1^1=1.5459,\ \lambda_1^2=4.2393,\ \lambda_1^3=$ -5.4527. $h_{2007}=$ -0.0755, $h_{2008}=$ -0.0849, $h_{2009}=$ -0.0440. The parameters of the RACM are: $\lambda_1^1=1.6618,\ \lambda_2^1=1.5884,\ \lambda_1^2=3.9215,\ \lambda_2^2=1.0818,\ \lambda_1^3=1.1141,\ \lambda_2^3=$ -243.8173, $\omega_1=0.5018,\ \omega_2=2.1087,\ p_{11}=0.8219,\ p_{22}=0.2516.,\ h_{2007}=$ -0.0097, $h_{2008}=$ -0.0088, $h_{2009}=$ -0.0084. The parameters of the real value are: $N_{2007}=18,\ N_{2008}=12,\ N_{2009}=13,\ h_{2007}=$ -0.0468, $h_{2008}=$ -0.0590, $h_{2009}=$ -0.0575.

Table 8: Pricing Errors of CAT Reinsurance under Alternative Intensity Models from 2007- 2009.

Model	Panel A Theoretical Values using Actual AMO and ΔCO_2		Panel B Theoretical Values using ARMA (1,1) for AMO and ΔCO_2	
	MAE	RMSE	MAE	RMSE
LM	1.4815	1.5661	1.4815	1.5662
LAM	1.0022	1.0896	0.8383	0.4725
LCM	0.8787	1.0881	1.0380	1.2170
LACM	0.8121	0.9521	0.8691	0.6297
RACM	0.5057	0.7127	0.4682	0.5542

The parameter values for base valuation are: $M=1,\ C=5,\ r_t=0.02,\ T=1,\ m=20,\ \alpha=0.129,\ \beta=0.168$. The parameters of the LM are: $\lambda_1^1=1.3808.\ h_{2007}=$ -0.0937, $h_{2008}=$ -0.0874, $h_{2009}=$ -0.0937. The parameters of the LAM are: $\lambda_1^1=1.3506,\ \lambda_1^2=4.1807,\ h_{2007}=$ -0.0755, $h_{2008}=$ -0.0849, $h_{2009}=$ -0.0437. The parameters of the LCM are: $\lambda_1^1=$ -0.7233, $\lambda_1^3=461.4121,,\ h_{2007}=$ -0.0933, $h_{2008}=$ -0.0884, $h_{2009}=$ -0.0649. The parameters of the LACM are: $\lambda_1^1=1.5459,\ \lambda_1^2=4.2393,\ \lambda_1^3=$ -5.4527. $h_{2007}=$ -0.0755, $h_{2008}=$ -0.0849, $h_{2009}=$ -0.0440. The parameters of the RACM are: $\lambda_1^1=1.6618,\ \lambda_2^1=1.5884,\ \lambda_1^2=3.9215,\ \lambda_2^2=1.0818,\ \lambda_1^3=1.1141,\ \lambda_2^3=$ -243.8173, $\omega_1=0.5018,\ \omega_2=2.1087,\ p_{11}=0.8219,\ p_{22}=0.2516.,\ h_{2007}=$ -0.0097, $h_{2008}=$ -0.0088, $h_{2009}=$ -0.0084. The parameters of the real value are: $N_{2007}=18,\ N_{2008}=12,\ N_{2009}=13,\ h_{2007}=$ -0.0468, $h_{2008}=$ -0.0590, $h_{2009}=$ -0.0575.

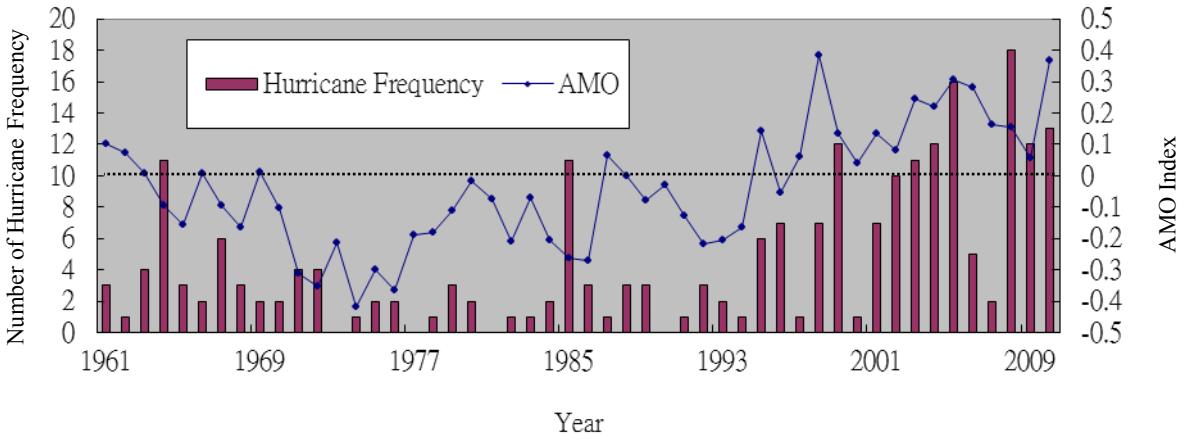

Figure 1: The AMO Index and Hurricane Frequency during 1961-2010

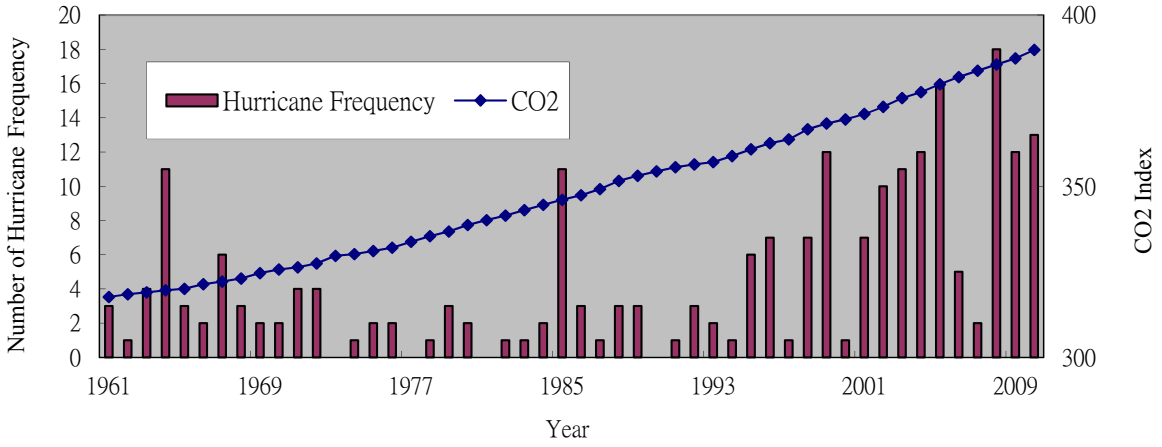

Figure 2: The CO_2 Index and Hurricane Frequency during 1961-2010

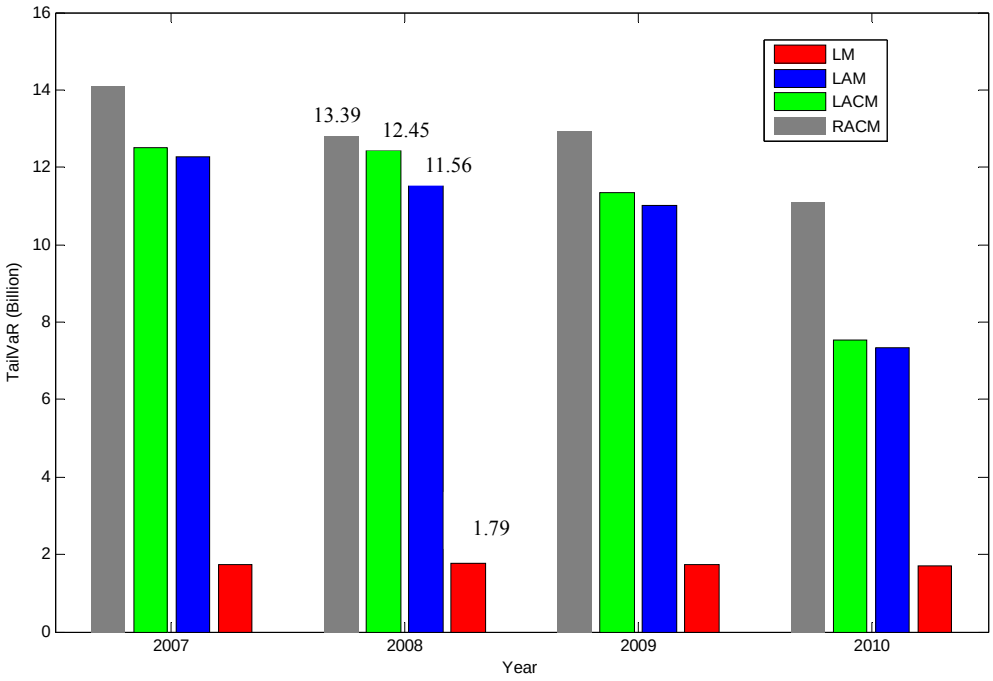

Figure 3: TailVaR in Linear and Regime-Switching Models.

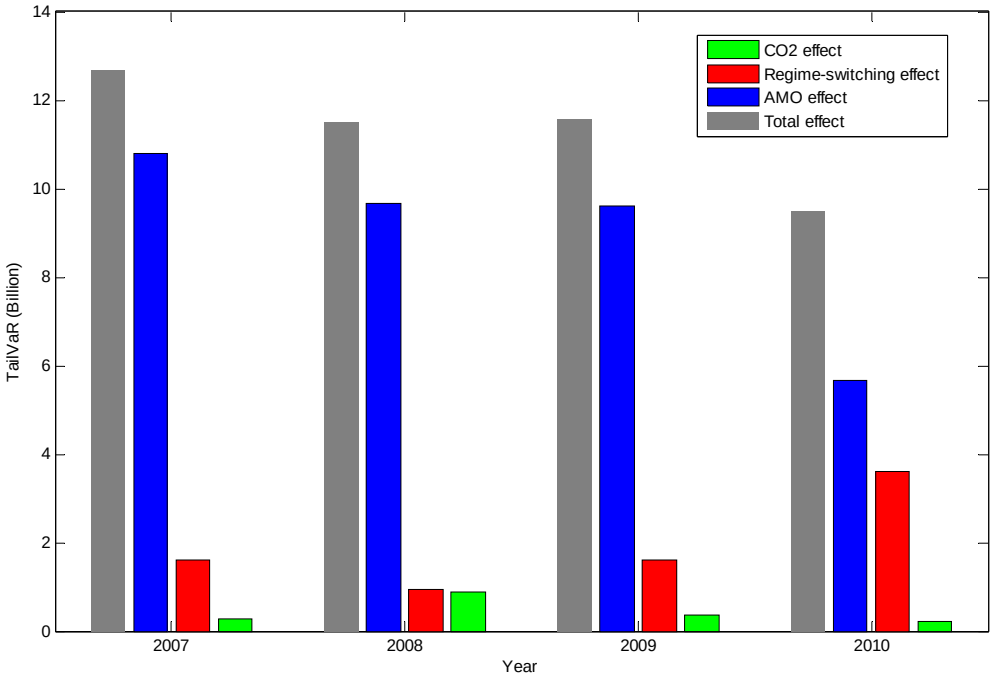

Figure 4: TailVaR: Regime-Switching Effect, CO_2 Effect and AMO Effect

References

1. Abate, J. and W. Whitt, (1992). Numerical inversion of probability generating functions. *Operations Research Letters*, 12, 245-251.
2. Barnett, T.P. et al., (2005). A Warning from warmer oceans. *Science,* 309, 284–287.
3. Bove, M. C., J. B. Elsner, C. W. Landsea, X.-F. Niu, and J. J. O'Brien, (1998). Effect of El Niño on U.S. landfalling hurricanes. revisited, *Bulletin of the American Meteorological Society*, 79, 2477.2482.
4. Chang, C.-C., S.-K Lin. and M.-T. Yu, (2011). Valuation of catastrophe equity puts with Markov-modulated Poisson processes. *Journal of Risk & Insurance*, 78(2), 447-473.
5. Cox, H., J. Fairchild and H. Pedersen, (2004). Valuation of structured risk management products. *Insurance: Mathematics and Economics*, 34, 259-272.
6. Christoffersen, P., R. Elkamhi, B. Feunou, and K. Jacobs, (2010). Option valuation with conditional heteroskedasticity and nonnormality. *Review of Financial Studies*, 23, 2139-2183.
7. Cummins, J. D. and H. Geman, (1995). Pricing catastrophe futures and call spreads: an arbitrage approach. *Journal of Fixed Income*, 4, 46-57.
8. Elliott, R. J., L. Chan, and T. K. Siu, (2005). Option pricing and Esscher transform under regime switching. *Annals of Finance*, 1, 423-432.
9. Emanuel, K., (2005). Increasing destructiveness of tropical cyclones over the past 30 years. *Nature*, 436, 686– 688.
10. Elsner, J. B., (2003). Tracking hurricanes. *Bulletin of the American Meteorological Society*, 84, 353-356
11. Elsner, J. B. and C. P., Schmertmann, (1993). Improving extended-range seasonal predictions of intense Atlantic hurricane activity. *Weather Forecasting,* 8, 345-351.
12. Elsner, J. B., Jagger, T. and X., Niu, (2000). Shifts in the rates of major hurricane activity over the North Atlantic during the 20th century. *Geophysical Research Letters*, 27, 1743-1746.
13. Elsner, J. B. and B. H., Bossak, (2004). Hurricane landfall probability and climate. Hurricanes and typhoons: past, present, and future, R. Murnane and K.-B. Liu, Eds., Columbia University Press, in press.
14. Elsner, J. B., B. H., Bossak and X.F., Niu, (2001). Secular changes to the ENSO-U.S.

hurricane relationship. *Geophysical Research Letters,* 28, 4123-4126.

15. Elsner, J. B. and T. H., Jagger, (2006). Prediction models for annual U.S. hurricanecounts. *American Meteorological Society,* 15, 2935-2952.
16. Elsner, J. B., T. H. Jagger, M. Dickinson and D. Rowe, (2008). Improving multiseason forecasts of North Atlantic hurricane activity. *American Meteorological Society,* 15, 1209-1219.
17. Esscher, J. B., (1932). On the probability function in the collective theory of risk. *Skandinavisk Aktuarietidskrift*, 15, 175-195.
18. Gerber, E. S. and W. Shiu, (1994). Option pricing by Esscher transforms. *Transactions of the Society of Actuaries XLVI*, 99-191.
19. Goldenberg, S. B., C.W. Landsea, A.M. Mestas-Nunez and W.M., Gray, (2001). The recent increase in Atlantic Hurricane activity：Causes and implication. *Science*, 293, 474-479.
20. Henderson-Sellers, A., Zhang, H., Berz, G., Emanuel, K., Gray, W., Landsea, C., Holland, G., Lighthill, J., Shieh, S.-L., Webster, P. and K., McGuffie, (1998). Tropical cyclones and global climate change: A post-IPCC assessment. *Bulletin of the American Meteorological Society,* 79, 19-38.
21. IPCC (2007) Climate Change 2007: The Physical Basis, Summary for Policymakers. Geneva.
22. Jagger, T. H., X. Niu and J.B., Elsner, (2002). A space-time model for seasonal hurricane prediction. *International Journal of Climatology,* 22, 451-465.
23. Jaimungal, S. and T. Wang, (2006). Catastrophe options with stochastic interest rates and compound Poisson losses. *Insurance: Mathematics and Insurances,* 38, 469-483.
24. Knutson T. R. and R. E. Tuleya, (2004). Impact of CO2-induced warming on simulated hurricane intensity and precipitation: sensitivity to the choice of climate model and convective parameterization. *Journal of Climate*, 17, 3477–3495.
25. Landsea, C. W., (2005). Hurricanes and global warming. *Nature*, 438, E11–E13.
26. Last, G., and A. Brandt, (1995). Marked point processes on the real line: The dynamic approach (New York: Springer-Verlag).
27. Lee, J.-P. and M.-T. Yu, (2002). Pricing default-risky CAT bonds with moral hazard and basis risk. *Journal of Risk and Insurance*, 69, 25-44.

28. Lehmiller, G. S., T. B. Kimberlain and J. B., Elsner, (1997). Seasonal prediction models for North Atlantic basin hurricane location. *Monthly Weather Review*, 125, 1780-1791.
29. Lin, S-K., C.-C. Chang, and M. R. Powers, (2009). The valuation of contingent capital with catastrophe risks, *Insurance: Mathematics and Economics*, 45, 65-73.
30. Louberge, H., E. Kellezi, and M. Gilli, (1999). Using catastrophe-linked securities to diversify insurance risk: a financial analysis of CAT bonds. *Journal of Risk and Insurance*, 22, 125-146.
31. Maloney, E. D., and D. L. Hartmann, (2000). Modulation of hurricane activity in the Gulf of Mexico by the Madden-Julian oscillation. *Science*, 287, 2002-4.
32. McDonnel, K. A. and N.J., Holbrook, (2004). A Poisson regression model of tropical cyclogenesis for the Australian-southwest Pacific Ocean region. *Weather Forecasting,* 19, 440-455.
33. Phillips, P.C.B and P., Perron, (1988). Testing for a unit root in time series regression. *Biometrika*, 75, 335-346.
34. Solow, A. R. and L.J., Moore, (2000). Testing for trend in North Atlantic hurricane activity, 1900-98. *Journal of Climate,* 15, 3111-3114.
35. Sutton, R. T. and D. L. R., Hodson, (2005). Atlantic Ocean forcing of North American and European summer climate. *Science*, 309, 115-118.
36. Webster, P. J. et al., (2005). Changes in tropical cyclone number, duration, and intensity in a warming environment. *Science,* 309, 1844–1846.
37. Webster, P. J. et al., (2006). Response to comment on climate in tropical cyclone number, duration, and intensity in a warming environment. *Science* 311, 1713.
38. Wu, Y.-C. and S.-L., Chung, (2010). Catastrophe risk management with counterparty risk using alternative instruments. *Insurance: Mathematics and Economics*, 47, 234-245.

Appendix A

This appendix illustrates the proof for the transition probability and a CAT loss under the risk-neutral measure. Let the Esscher transform is as follows:

$$\frac{dQ(y_1^Q \in dy_1, y_2^Q \in dy_2, ..., y_m^Q \in dy_m,\ N_{t,S_t}^Q = m,\ S_{t-1} = i,\ S_t = j)}{dP(y_1 \in dy_1, y_2 \in dy_2, ..., y_m \in dy_m,\ N_{t,S_t} = m,\ S_{t-1} = i,\ S_t = j)} = \frac{e^{h_t \sum_{n=1}^{m} y_n}}{E^P\left(e^{h_t \sum_{n=N_{t-1,S_t}}^{N_{t,S_t}} y_n}\right)}, \qquad \text{(A.1)}$$

Because that the CAT loss and the transition probability is independent, hence (A.1) can be rewritten as follows:

$$dQ(y_1^Q \in dy_1, y_2^Q \in dy_2, ..., y_m^Q \in dy_m,\ N_{t,S_t}^Q = m,\ S_{t-1} = i,\ S_t = j)$$

$$= dP(y_1 \in dy_1) \times dP(y_2 \in dy_2) \times ... \times dP(y_m \in dy_m) \times dP(N_{t,S_t} = m,\ S_{t-1} = i,\ S_t = j) \frac{e^{h_t \sum_{n=1}^{m} y_n}}{E^P\left(e^{h_t \sum_{n=N_{t-1,S_t}}^{N_{t,S_t}} y_n}\right)}$$

$$= \frac{e^{h_t y_1}}{\phi_t(h_t)} f(y_1) \times \frac{e^{h_t y_2}}{\phi_t(h_t)} f(y_2) \times ... \times \frac{e^{h_t y_m}}{\phi_t(h_t)} f(y_m) \times P(m,1) \frac{\phi_t(h_t)^m}{E^P\left(e^{h_t \sum_{n=N_{t-1,S_t}}^{N_{t,S_t}} y_n}\right)}.$$

Thus, we can let $f^Q(y_n) = \frac{e^{h_t y_n}}{\phi_t(h_t)} f(y_n)$ and $Q(m,1) = P(m,1) \frac{\phi_t(h_t)^m}{E^P\left(e^{h_t \sum_{n=N_{t-1,S_t}}^{N_{t,S_t}} y_n}\right)}$ to obtain the new probability density function $f^Q(y_n)$ and the new transition probability $Q(m,1)$ under the risk-neutral probability measure. For the new regime switching Poisson process N_{t,S_t} and the matrix of the transition rates Θ under the risk-neutral probability measure, we let $\mathrm{Q(m,1)} = \left(\phi_t(h_t)\right)^m \exp\left(-\Lambda(\phi_t(h_t)-1)\right)\mathrm{P(m,1)}$, and thus we have

$$Q^*(z,1)=\sum_{m=0}^{\infty}\mathrm{Q(m,1)}\,z^m=\sum_{m=0}^{\infty}\left(\phi_t(h_t)\right)^m\exp\left(-\Lambda(\phi_t(h_t)-1)\right)\mathrm{Q(m,1)}\,z^m$$

$$=\sum_{m=0}^{\infty}(z\phi_t(h_t))^m\exp(-\Lambda(\phi_t(h_t)-1))\mathrm{Q(m,1)}.$$

The unique solution of $Q^*(z,1)$ is:

$$Q^*(z,1)=\exp\left[\ \Theta-\left(1-(z\,\phi_t(h_t))\Lambda\right]\times\exp\left[-\Lambda(\phi_t(h_t)-1)\right]=\exp\left[\Theta-((1-z)\,\phi_t(h_t)\Lambda)\right].$$

Hence, the new regime switching Poisson process N_{t,S_t} has the new intensity matrix $\Lambda^Q=\Lambda\phi_t(h_t)$ of weather-induced events and the matrix of the transition rates Θ remains unchanged under the risk-neutral probability measure.

Appendix B

$$V(0)=\sum_{t=1}^{T}e^{-r_t}E_{t-1}^{Q}\left[(Y_{t,S_t}-Y_{t-1,S_{t-1}}-M)^+-(Y_{t,S_t}-Y_{t-1,S_{t-1}}-C)^+\right],S_t=\{1,2\},$$

$$=\sum_{t=1}^{T}e^{-r_t}\,E_{t-1}^{Q}\left[(Y_{t,S_t}-Y_{t-1,S_t}-M)^+\right]-\sum_{t=1}^{T}e^{-r_t}\,E_{t-1}^{Q}\left[(Y_{t,S_t}-Y_{t-1,S_t}-C)^+\right]=A-B,$$

where

$$\mathrm{A}=\sum_{t=1}^{T}e^{-r_t}\,E_{t-1}^{Q}\left[(Y_{t,S_t}-Y_{t-1,S_t}-M)^+\right]$$

$$=\sum_{t=1}^{T}e^{-r_t}\,E_{t-1}^{Q}\left[(\sum_{n=N_{t-1,S_t}}^{N_{t,S_t}}y_n-M)\times 1_{\left\{\sum_{n=N_{t-1,S_t}}^{N_{t,S_t}}y_n>M\right\}}\right]$$

$$=\sum_{t=1}^{T}e^{-r_t}\int_M^{\infty}y_t^m f^Q(y_t^m\left|N_{t,S_t}-N_{t-1,S_t}=m\right.)\sum_{m=0}^{\infty}\mathrm{Prob}(N_{t,S_t}-N_{t-1,S_t}=m)\,dy_t^m$$

$$=\sum_{t=1}^{T}e^{-r_t}\sum_{m=0}^{\infty}\sum_{i}^{2}\sum_{j}^{2}\pi_i\,Q_{ij}(m,1)\int_M^{\infty}y_t^m f^Q(y_t^m\left|N_{t,S_t}-N_{t-1,S_t}=m\right.)dy_t^m \qquad \text{(B.1)}$$

Since that $f^Q(y_t)=\dfrac{e^{h_t y_t}}{\phi_t(h_t)}f(y_t)$ and y stands for the gamma distribution with shape parameter α and scale parameter β, we have

$$f^{Q}(y_t) = \frac{(\beta - h_t)^{\alpha}}{\Gamma(\alpha)}(y)^{\alpha-1}e^{-(\beta-h_t)y}.$$

$y_t^m = \sum_{n=1}^{m} y_n$ represents the total losses of m insured CAT claims under the risk-neutral probability measure Q and stands for the gamma distribution with shape parameter αm and scale parameter β with the density function $f^{Q}(y_t^m) = \frac{(\beta - h_t)^{\alpha m}}{\Gamma(\alpha m)}(y_t^m)^{\alpha m-1}e^{-(\beta-h_t)y_t^m}$. And we have $\lambda_{t,S_t}^{Q} = \lambda_{t,S_t}\phi(h_t) = \lambda_{t,i}^{Q} = \mathrm{e}^{\lambda_i^1+\lambda_i^2 AMO_t^* + \lambda_i^3 CO_{2,t}^*}(1-\frac{h_t}{\beta})$. Hence, we have

$$\int_M^{\infty}(y_t^m - M)f^{Q}(y_t^m)dy_t^m = \int_M^{\infty} y_t^m \; f^{Q}(y_t^m)dy_t^m - \; M\int_M^{\infty} f^{Q}(y_t^m)dy_t^m .$$

Since that $\int_M^{\infty} y_t^m \; f^{Q}(y_t^m)dy_t^m = \int_0^{\infty} y_t^m \; f^{Q}(y_t^m)dy_t^m - \int_0^{M} y_t^m \; f^{Q}(y_t^m)dy_t^m$

and $y_t^m \; f^{Q}(y_t^m) = y_t^m \; \frac{(\beta - h_t)^{\alpha m}}{\Gamma(\alpha m)}(y_t^m)^{\alpha m-1}e^{-(\beta-h_t)y_t^m}$

$$= \frac{\Gamma(\alpha m+1)}{(\beta - h_t)\Gamma(\alpha m)}\left(\frac{(\beta - h_t)^{\alpha m+1}}{\Gamma(\alpha m+1)}(y_t^m)^{(\alpha m+1)-1}e^{-(\beta-h_t)y_t^m}\right),$$

we have $\int_0^{\infty} y_t^m \; \frac{(\beta - h_t)^{\alpha m}}{\Gamma(\alpha m)}(y_t^m)^{\alpha m-1}e^{-(\beta-h_t)y_t^m} = \frac{\Gamma(\alpha m+1)}{(\beta - h_t)\Gamma(\alpha m)} = \frac{\alpha m}{(\beta - h_t)}$.

Similar, we obtain

$$\int_0^{M} y_t^m f^{Q}(y_t^m)dy_t^m = \frac{\Gamma(\alpha m+1)}{(\beta - h)\Gamma(\alpha m)}\int_0^{M}\frac{(\beta - h_t)^{\alpha m+1}}{\Gamma(\alpha m+1)}(y_t^m)^{(\alpha m+1)-1}e^{-(\beta-h_t)y_t^m}dy_t^m$$
$$= \frac{\alpha m}{(\beta - h_t)}\;\frac{\gamma(\alpha m+1,(\beta - h_t)M)}{\Gamma(\alpha m+1)}$$

Hence, $\int_M^{\infty} y_t^m \; f^{Q}(y_t^m)dy_t^m = \frac{\alpha m}{(\beta - h_t)}\left(1-\frac{\gamma(\alpha m+1,(\beta - h_t)M)}{\Gamma(\alpha m+1)}\right)$,

and $M\int_M^{\infty} \; f^{Q}(y_t^m)dy_t^m = M\int_0^{\infty} f^{Q}(y_t^m)dy_t^m - M\int_0^{M} \; f^{Q}(y_t^m)dy_t^m = \mathrm{M}\left(1-\frac{\gamma(\alpha m,(\beta - h_t)M)}{\Gamma(\alpha m)}\right)$.

Therefore, the computation of part B is similar to part A, thus we have

$$V(0) = \sum_{t=1}^{T} e^{-r_t}\sum_{m=0}^{\infty}\sum_{i}^{2}\sum_{j}^{2}\pi_i \, Q_{ij}(m,1)\left[\int_M^{\infty}(y_{t,j}^m - M)f^{Q}(y_t^m)dy_t^m - \int_C^{\infty}(y_t^m - C)f^{Q}(y_t^m)dy_t^m\right].$$